

Locking-free Thick-Thin Rod/Beam Element Based on a von Karman Type Nonlinear Theory in Rotated Reference Frames For Large Deformation Analyses of Space-Frame Structures

H.H. Zhu¹, Y.C. Cai^{1,2}, J.K. Paik³ and S.N. Atluri⁴

Abstract: This paper presents a new shear flexible beam/rod element for large deformation analyses of space-frame structures, comprising of thin or thick beams. The formulations remain uniformly valid for thick or thin beams, without using any numerical expediences such as selective reduced integrations, etc. A von Karman type nonlinear theory of deformation is employed in the co-rotational reference frame of the present beam element, to account for bending, stretching, torsion and shearing of each element. Transverse shear strains in two independent directions are introduced as additional variables, in order to eliminate the shear locking phenomenon. An assumed displacement approach is used to derive an explicit expression for the (16x16) *symmetric* tangent stiffness matrix of the beam element in the co-rotational reference frame. Numerical examples demonstrate that the present element is free from shear locking and is suitable for the large deformation analysis of spaced frames with thick/thin members. Significantly, this paper provides a text-book example of an explicit expression for the (16x16) *symmetric tangent stiffness matrix* of a finitely deforming beam element, which can be employed in very simple analyses of large deformations of space-frames. The present methodologies can be extended to study the very large deformations of plates and shells as well, and can be shown to be theoretically valid for thick or thin plates and shells, without using selective reduced integrations and without the need for stabilizing the attendant zero-energy modes.

¹ Key Laboratory of Geotechnical and Underground Engineering of Ministry of Education, Department of Geotechnical Engineering, Tongji University, Shanghai 200092, P.R.China

² Corresponding author. Email: yc_cai@163.net. Key Laboratory for the Exploitation of Southwest Resources and Environmental Disaster Control Engineering, Ministry of Education, Chongqing University, Chongqing 400044, P.R.China.

³ Lloyd's Register Educational Trust (The LRET) Research Center of Excellence, Pusan National University, Korea

⁴ Center for Aerospace Research & Education, University of California, Irvine

Keywords: Large deformation, Thick Beam, Thick Rod, Locking, Explicit tangent stiffness, Updated Lagrangian formulation, Space frames

1 Introduction

Exact and efficient nonlinear large deformation analyses of space frames have attracted much attention due to their significance in diverse engineering applications, such as civil and aerospace engineering, and tensegrity structures in biological applications. In the past decades, many different methods were developed by numerous researchers for the geometrically nonlinear analyses of 3D frame structures. Bathe and Bolourchi (1979) employed the total Lagrangian and updated Lagrangian approaches to formulate fully nonlinear 3D continuum beam elements. Punch and Atluri (1984) examined the performance of linear and quadratic Serendipity hybrid-stress 2D and 3D beam elements. Based on geometric considerations, Lo (1992) developed a general 3D nonlinear beam element, which can remove the restriction of small nodal rotations between two successive load increments. Kondoh, Tanaka and Atluri (1986), Kondoh and Atluri (1987), Shi and Atluri (1988) presented the derivations of explicit expressions of the tangent stiffness matrix, without employing either numerical or symbolic integration. Zhou and Chan (2004a, 2004b) developed a precise element capable of modeling elastoplastic buckling of a column by using a single element per member for large deflection analysis. Izzuddin (2001) clarified some of the conceptual issues which are related to the geometrically nonlinear analysis of 3D framed structures. Simo (1985), Mata, Oller and Barbat (2007, 2008), Auricchio, Carotenuto and Reali (2008) considered the nonlinear constitutive behavior in the geometrically nonlinear formulation for beams. Iura and Atluri (1988), Chan (1994), Xue and Meek (2001), Wu, Tsai and Lee (2009) studied the nonlinear dynamic response of the 3D frames. Lee, Lin, Lee, Lu and Liu (2008), Lee, Lu, Liu and Huang (2008) gave the exact large deflection solutions of the beams for some special cases. Atluri and Zhu (1998), Zhu, Zhang and Atluri (1999), Wen and Hon (2007); Dinis, Jorge and Belinha (2009), Han, Rajendran and Atluri (2005), Lee and Chen (2009) applied meshless methods to the analyses of nonlinear problems with large deformations or rotations. Gendy and Saleeb (1992), Atluri, Iura, and Vasudevan (2001) had brief discussions of the frames with arbitrary cross sections. Large rotations in beams, plates and shells, and attendant variational principles involving the rotation tensor as a direct variable, were studied extensively by Atluri and his co-workers (see, for instance, Atluri 1980, Atluri 1984, and Atluri and Cazzani 1994).

In Cai, Paik and Atluri (2009a), a simple “thin” beam/rod element, based on simple mechanics and physical clarity, for geometrically nonlinear large rotation analyses of space frames consisting of “thin” beam members of arbitrary cross-section, has

been proposed. This thin element formulation lead to an explicit expression of the (12×12) *symmetric* tangent stiffness matrix. However, the element is only accurate in very thin structures because the influence of the shear deformation has been neglected. The neglect of the effect of the shear deformation may impair the computational accuracy and may lead to the error of results for moderately thick structures. Researchers had developed many shear-flexible beam elements (Reddy 1997; Mukherjee and Prathap 2001; Atluri, Cho and Kim 1999; Zhang and Di 2003; Li 2007) to obtain the acceptable results for a wide range of element thicknesses, and successful applied them to diverse engineering fields. Nevertheless, these methods will involve very complex algebraic derivations when they are extended to the large deformation analysis of structures. In this paper, a new shear flexible beam/rod element is proposed for large deformation analyses of space-frame structures consisting of thick or thin members. A von Karman type nonlinear theory of deformation is employed in the co-rotational reference frame of the present beam element, to account for bending, stretching, torsion and shearing of each element. Transverse shear strains in two independent directions are introduced to eliminate the shear locking phenomenon in the shear flexible beam elements, thus, the present formulations remain uniformly valid for either thick or thin beams, without using the numerical expediciencies of selective reduced integrations and without the need for stabilizing the attendant zero-energy modes. An assumed displacement approach is used to derive an explicit expression for the (16×16) *symmetric* tangent stiffness matrix of the beam element in the co-rotational reference frame. Numerical examples demonstrate that the present element is free from shear locking and is suitable for the large deformation analysis of thick/thin spaced frames. Significantly, this paper provides a text-book example of an explicit expression for the (16×16) *symmetric tangent stiffness matrix* of a finitely deforming beam element, which can be employed in very simple analyses of large deformations of space-frames consisting of either thick or thin members. The present methodologies can be extended to study the very large deformations of plates and shells as well, and can be shown to be theoretically valid for thick or thin plates and shells (Sladek, Sladek, Sulek and Atluri 2008; Majorana and Salomoni 2008; Gato and Shie 2008; Kulikov and Plotnikova 2008), without using selective reduced integrations and without the need for stabilizing the attendant zero-energy modes.

Similar to Cai, Paik and Atluri (2010a), the present beam element including the shear influence has a much simpler form than those based on exact continuum theories of Simo (1985) and Bathe and Bolourchi (1979). The present explicit derivation of the tangent stiffness matrix of a finitely deforming beam of an arbitrary cross-section is more general and much simpler than in the earlier papers of Kondoh, Tanaka and Atluri (1986), Kondoh and Atluri (1987), and Shi and Atluri

(1988). Furthermore, unlike in the formulations of Simo(1985), Crisfield (1990) [and many others who followed them], which lead to the currently popular myth that the stiffness matrices of finitely rotated structural members should be *unsymmetric*, the (16x16) stiffness matrix of the beam element in the present paper is enormously simple, and remains *symmetric* throughout the finite rotational deformation.

2 Von-Karman type nonlinear theory including shear deformation for a rod with large deformations

We consider a fixed global reference frame with axes \bar{x}_i ($i = 1, 2, 3$) and base vectors $\bar{\mathbf{e}}_i$. An initially straight rod of an arbitrary cross-section and base vectors $\tilde{\mathbf{e}}_i$, in its undeformed state, with local coordinates \tilde{x}_i ($i = 1, 2, 3$), is located arbitrarily in space, as shown in Fig.1. The current configuration of the rod, after arbitrarily large deformations (but small strains) is also shown in Fig.1.

The local coordinates in the reference frame in the current configuration are x_i and the base vectors are \mathbf{e}_i ($i = 1, 2, 3$). The nodes 1 and 2 of the rod (or an element of the rod) are supposed to undergo arbitrarily large displacements, and the rotations between the $\tilde{\mathbf{e}}_i$ ($i = 1, 2, 3$) and the \mathbf{e}_k ($k = 1, 2, 3$) base vectors are assumed to be arbitrarily finite. In the continuing deformation from the current configuration, the local displacements in the x_i (\mathbf{e}_i) coordinate system are assumed to be moderate, and the local gradient ($\partial u_{10}/\partial x_1$) is assumed to be small compared to the transverse rotations ($\partial u_{\alpha 0}/\partial x_1$) ($\alpha = 2, 3$). Thus, in essence, a von-Karman type deformation is assumed for the continued deformation from the current configuration, in the corotational frame of reference \mathbf{e}_i ($i = 1, 2, 3$) in the local coordinates x_i ($i = 1, 2, 3$). If H is the characteristic dimension of the cross-section of the rod, the precise assumptions governing the continued deformations from the current configuration are

$$\frac{u_{10}}{H} \ll 1; \quad \frac{H}{L} \text{ need not be } \leq 1.$$

$$\frac{u_{\alpha 0}}{H} \approx O(1) \quad (\alpha = 2, 3)$$

$$\frac{\partial u_{10}}{\partial x_1} \ll \frac{\partial u_{\alpha 0}}{\partial x_1} \quad (\alpha = 2, 3)$$

and $\left(\frac{\partial u_{\alpha 0}}{\partial x_1}\right)^2$ ($\alpha = 2, 3$) are not negligible.

As shown in Fig.2, we consider the large deformations of a cylindrical rod, subjected to bending (in two directions), and torsion around x_1 . The cross-section is unsymmetrical around x_2 and x_3 axes, and is constant along x_1 .

As shown in Fig.2, the warping displacement due to the torque T around x_1 axis is $u_{1T}(x_2, x_3)$ and does not depend on x_1 , the axial displacement at the origin ($x_2 = x_3 = 0$) is $u_{10}(x_1)$, and the bending displacement at $x_2 = x_3 = 0$ along the axis x_1 are $u_{20}(x_1)$ (along x_2) and $u_{30}(x_1)$ (along x_3).

We consider only loading situations when the generally 3-dimensional displacement state in the \mathbf{e}_i system, denoted as

$$u_i = u_i(x_k) \quad i = 1,2,3; k = 1,2,3$$

is simplified to be of the type:

$$\begin{aligned} u_1 &= u_{1T}(x_2, x_3) + u_{10}(x_1) - x_2\theta_2 - x_3\theta_3 \\ u_2 &= u_{20}(x_1) - \theta_1 x_3 \\ u_3 &= u_{30}(x_1) + \theta_1 x_2 \end{aligned} \tag{1}$$

where θ_1 is the total torsion of the rod at x_1 due to the torque T , θ_2 is the total rotation around x_3 , and θ_3 is the total rotation around x_2 , where θ_2 and θ_3 include the influence of the shear deformation.

2.1 Strain-displacement relations

Considering only von Karman type nonlinearities in the rotated reference frame $\mathbf{e}_i(x_i)$, we can write the Green-Lagrange strain-displacement relations in the updated Lagrangian co-rotational frame \mathbf{e}_i in Fig.1 as:

$$\begin{aligned} \epsilon_{11} &= \frac{\partial u_1}{\partial x_1} + \frac{1}{2} \left(\frac{\partial u_2}{\partial x_1} \right)^2 + \frac{1}{2} \left(\frac{\partial u_3}{\partial x_1} \right)^2 \\ &= \frac{\partial u_{10}}{\partial x_1} + \frac{1}{2} \left(\frac{\partial u_{20}}{\partial x_1} \right)^2 + \frac{1}{2} \left(\frac{\partial u_{30}}{\partial x_1} \right)^2 - x_2 \frac{\partial \theta_2}{\partial x_1} - x_3 \frac{\partial \theta_3}{\partial x_1} \\ \epsilon_{12} &= \frac{1}{2} \left(\frac{\partial u_1}{\partial x_2} + \frac{\partial u_2}{\partial x_1} \right) = \frac{1}{2} \left(\frac{\partial u_{1T}}{\partial x_2} - \frac{\partial \theta_1}{\partial x_1} x_3 + \frac{\partial u_{20}}{\partial x_1} - \theta_2 \right) \\ \epsilon_{13} &= \frac{1}{2} \left(\frac{\partial u_1}{\partial x_3} + \frac{\partial u_3}{\partial x_1} \right) = \frac{1}{2} \left(\frac{\partial u_{1T}}{\partial x_3} + \frac{\partial \theta_1}{\partial x_1} x_2 + \frac{\partial u_{30}}{\partial x_1} - \theta_3 \right) \\ \epsilon_{22} &= \frac{\partial u_2}{\partial x_2} + \frac{1}{2} \left(\frac{\partial u_1}{\partial x_2} \right)^2 + \frac{1}{2} \left(\frac{\partial u_2}{\partial x_2} \right)^2 + \frac{1}{2} \left(\frac{\partial u_3}{\partial x_2} \right)^2 \approx 0 \\ \epsilon_{23} &\approx 0 \\ \epsilon_{33} &\approx 0 \end{aligned} \tag{2}$$

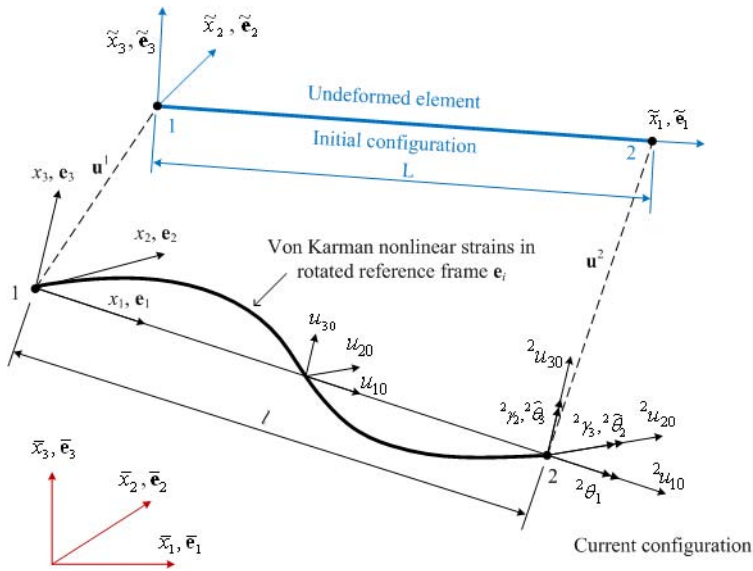


Figure 1: Kinematics of deformation of a space framed member

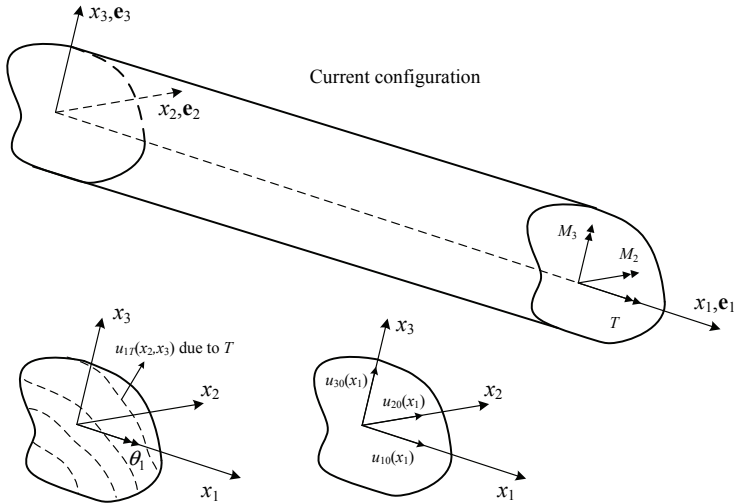


Figure 2: Large deformation analysis model of a cylindrical rod

By letting

$$\theta'_1 = \theta_{1,1}$$

$$\gamma_2 = u_{20,1} - \theta_2$$

$$\gamma_3 = u_{30,1} - \theta_3$$

$$\chi_{22} = -u_{20,11}$$

$$\chi_{33} = -u_{30,11}$$

$$\epsilon_{11}^0 = u_{10,1} + \frac{1}{2} (u_{20,1})^2 + \frac{1}{2} (u_{30,1})^2 = \epsilon_{11}^{0L} + \epsilon_{11}^{0N}$$

(3)

the strain-displacement relations can be rewritten as

$$\begin{aligned}
 \varepsilon_{11} &= \varepsilon_{11}^0 + x_2 \chi_{22} + x_3 \chi_{33} + x_2 \gamma_{2,1} + x_3 \gamma_{3,1} \\
 \varepsilon_{12} &= \frac{1}{2} (u_{1T,2} - \theta'_1 x_3 + \gamma_2) \\
 \varepsilon_{13} &= \frac{1}{2} (u_{1T,3} + \theta'_1 x_2 + \gamma_3) \\
 \varepsilon_{22} &= \varepsilon_{33} = \varepsilon_{23} = 0
 \end{aligned} \tag{4}$$

where , i denotes a differentiation with respect to x_i .

The matrix form of the Eq.(4) is

$$\varepsilon = \varepsilon^{Lb} + \varepsilon^{Ls} + \varepsilon^N = \varepsilon^L + \varepsilon^N \tag{5}$$

where ε^{Lb} is the linear part of the bending strain, ε^N is the nonlinear part of the bending strain, ε^{Ls} is the shear strain, and

$$\varepsilon^{Lb} = \begin{Bmatrix} \varepsilon_{11}^{Lb} \\ \varepsilon_{12}^{Lb} \\ \varepsilon_{13}^{Lb} \end{Bmatrix} = \begin{Bmatrix} u_{10,1} + x_2 \chi_{22} + x_3 \chi_{33} \\ \frac{1}{2} (u_{1T,2} - \theta'_1 x_3) \\ \frac{1}{2} (u_{1T,3} + \theta'_1 x_2) \end{Bmatrix} \tag{6}$$

$$\varepsilon^{Ls} = \begin{Bmatrix} \varepsilon_{11}^{Ls} \\ \varepsilon_{12}^{Ls} \\ \varepsilon_{13}^{Ls} \end{Bmatrix} = \begin{Bmatrix} x_2 \gamma_{2,1} + x_3 \gamma_{3,1} \\ \gamma_2 / 2 \\ \gamma_3 / 2 \end{Bmatrix} \tag{7}$$

$$\varepsilon^N = \begin{Bmatrix} \varepsilon_{11}^N \\ \varepsilon_{12}^N \\ \varepsilon_{13}^N \end{Bmatrix} = \begin{Bmatrix} \frac{1}{2} (u_{20,1})^2 + \frac{1}{2} (u_{30,1})^2 \\ 0 \\ 0 \end{Bmatrix} \tag{8}$$

From Eqs.(3) and (4), it is seen that in the present formulation, the transverse displacements (u_{20} and u_{30}) as well as the transverse shear strains (γ_2 and γ_3) are retained as independent variables. This type of formulation has been clearly shown (Atluri 2005) to lead to be locking-free and remains uniformly valid for either thick or thin beams, without using such numerical gimmicks as selective/reduced integrations and without the need for stabilizing the attendant spurious modes of zero-energy. On the other hand, one may also use formulations wherein the transverse displacements (u_{20} and u_{30}) as well as the total rotations (θ_2 and θ_3) are retained as independent variables. However, it has been simply explained in (Atluri 2005), how such formulations lead to locking, thus necessitating the use of selective reduced integration and the need for the stabilization of the attendant zero-energy modes.

2.2 Stress-Strain relations

Taking the material to be linear elastic, we assume that the additional second Piola-Kirchhoff stress, denoted by tensor \mathbf{S}^1 in the updated Lagrangian co-rotational reference frame \mathbf{e}_i of Fig.1 (in addition to the pre-existing Cauchy stress due to prior deformation, denoted by τ^0), is given by:

$$\begin{aligned} S_{11}^1 &= E \varepsilon_{11} \\ S_{12}^1 &= 2\mu \varepsilon_{12} \\ S_{13}^1 &= 2\mu \varepsilon_{13} \\ S_{22}^1 &= S_{33}^1 = S_{23}^1 \approx 0 \end{aligned} \quad (9)$$

where $\mu = \frac{E}{2(1+\nu)}$; E is the elastic modulus; ν is the Poisson ratio.

By using Eq.(5), Eq.(9) can also be written as

$$\mathbf{S}^1 = \tilde{\mathbf{D}} \left(\varepsilon^{Lb} + \varepsilon^{Ls} + \varepsilon^N \right) = \mathbf{S}^{Lb} + \mathbf{S}^{Ls} + \mathbf{S}^N = \mathbf{S}^{1L} + \mathbf{S}^{1N} \quad (10)$$

where

$$\tilde{\mathbf{D}} = \begin{bmatrix} E & 0 & 0 \\ 0 & 2\mu & 0 \\ 0 & 0 & 2\mu \end{bmatrix} \quad (11)$$

From Eq.(4) and Eq.(9), the generalized nodal forces of the rod element in Fig.1

can be written as

$$\begin{aligned}
N_{11} &= \int_A S_{11}^1 dA = E \left(A\varepsilon_{11}^0 + \chi_{22} \int_A x_2 dA + \chi_{33} \int_A x_3 dA + \gamma_{2,1} \int_A x_2 dA + \gamma_{3,1} \int_A x_3 dA \right) \\
&= E (A\varepsilon_{11}^0 + I_2\chi_{22} + I_3\chi_{33} + I_2\gamma_{2,1} + I_3\gamma_{3,1}) \\
M_{33} &= \int_A S_{11}^1 x_3 dA = E \int_A (\varepsilon_{11}^0 + x_2\chi_{22} + x_3\chi_{33} + x_2\gamma_{2,1} + x_3\gamma_{3,1}) x_3 dA \\
&= E (I_3\varepsilon_{11}^0 + I_{23}\chi_{22} + I_{33}\chi_{33} + I_{23}\gamma_{2,1} + I_{33}\gamma_{3,1}) \\
M_{22} &= \int_A S_{11}^1 x_2 dA = E \int_A (\varepsilon_{11}^0 + x_2\chi_{22} + x_3\chi_{33} + x_2\gamma_{2,1} + x_3\gamma_{3,1}) x_2 dA \\
&= E (I_2\varepsilon_{11}^0 + I_{22}\chi_{22} + I_{23}\chi_{33} + I_{22}\gamma_{2,1} + I_{23}\gamma_{3,1}) \\
T &= \int_A S_{13}^1 x_2 - S_{12}^1 x_3 dA = 2\mu \int_A (x_2\varepsilon_{13} - x_3\varepsilon_{12}) dA \\
&= \frac{2\mu}{2} \int_A [(u_{1T,3} + \theta_1' x_2 + \gamma_3) x_2 - (u_{1T,2} - \theta_1' x_3 + \gamma_2) x_3] dA \\
&= \mu \int_A \theta_1' (x_2^2 + x_3^2) dA + \mu \int_A (\gamma_3 x_2 - \gamma_2 x_3) dA + \mu \int_A (u_{1T,3} x_2 - u_{1T,2} x_3) dA \\
&= \mu I_{rr} \theta_1' + \mu I_2 \gamma_3 - \mu I_3 \gamma_2 + \mu \oint_S (u_{1T} n_3 x_2 - u_{1T} n_2 x_3) dS \\
&= \mu I_{rr} \theta_1' + \mu I_2 \gamma_3 - \mu I_3 \gamma_2 \\
Q_{12} &= \int_A S_{12}^1 dA = \mu \int_A (u_{1T,2} - \theta_1' x_3 + \gamma_2) dA \approx \mu (-I_3 \theta_1' + A\gamma_2) \\
Q_{13} &= \int_A S_{13}^1 dA = \mu \int_A (u_{1T,3} + \theta_1' x_2 + \gamma_3) dA
\end{aligned} \tag{12}$$

where n_j is the outward normal, $I_2 = \int_A x_2 dA$, $I_3 = \int_A x_3 dA$, $I_{33} = \int_A x_3^2 dA$, $I_{22} = \int_A x_2^2 dA$, $I_{23} = \int_A x_2 x_3 dA$, and $I_{rr} = \int_A (x_2^2 + x_3^2) dA$.

The matrix form of the above equations is

$$\boldsymbol{\sigma} = \mathbf{DE} \tag{13}$$

where

$$\boldsymbol{\sigma} = \begin{Bmatrix} \sigma_1 \\ \sigma_2 \\ \sigma_3 \\ \sigma_4 \\ \sigma_5 \\ \sigma_6 \end{Bmatrix} = \begin{Bmatrix} N_{11} \\ M_{22} \\ M_{33} \\ T \\ Q_{12} \\ Q_{13} \end{Bmatrix} = \text{element generalized stresses} \tag{14}$$

$$\mathbf{E} = \mathbf{E}^L + \mathbf{E}^N = \begin{Bmatrix} E_1 \\ E_2 \\ E_3 \\ E_4 \\ E_5 \\ E_6 \end{Bmatrix} = \text{element generalized strains} \tag{15}$$

$$\mathbf{D} = \begin{bmatrix} EA & EI_2 & EI_3 & 0 & 0 & 0 \\ EI_2 & EI_{22} & EI_{23} & 0 & 0 & 0 \\ EI_3 & EI_{23} & EI_{33} & 0 & 0 & 0 \\ 0 & 0 & 0 & \mu I_{rr} & -\mu I_3 & \mu I_2 \\ 0 & 0 & 0 & -\mu I_3 & \mu kA & 0 \\ 0 & 0 & 0 & \mu I_2 & 0 & \mu kA \end{bmatrix} \tag{16}$$

where k is the shear coefficient related to the cross section, e.g., k is taken to be $2/3$ for the rectangular cross sections and k is taken to be 1.0 for the asymmetric cross sections in this paper.

$$\mathbf{E}^L = [u_{10,1} \quad -u_{20,11} + \gamma_{2,1} \quad -u_{30,11} + \gamma_{3,1} \quad \theta_{1,1} \quad \gamma_2 \quad \gamma_3]^T \tag{17}$$

$$\mathbf{E}^N = \left[\frac{1}{2} (u_{20,1}^2 + u_{30,1}^2) \quad 0 \quad 0 \quad 0 \quad 0 \quad 0 \right]^T \tag{18}$$

3 Updated Lagrangian formulation in the co-rotational reference frame \mathbf{e}_i

3.1 Interpolation functions

As shown in Fig.1, the rod element has two nodes with 8 degrees of freedom per node. By defining the following shape functions

$$\phi_1 = 1 - \xi, \phi_2 = \xi \tag{19}$$

$$\begin{aligned} N_1 &= 1 - 3\xi^2 + 2\xi^3, N_3 = 3\xi^2 - 2\xi^3 \\ N_2 &= (\xi - 2\xi^2 + \xi^3) l, N_4 = (\xi^3 - \xi^2) l \end{aligned} \tag{20}$$

where l is the length of the rod element,

$$\xi = \frac{x_1 - {}^1x_1}{l} \quad (0 < \xi < 1)$$

and 1x_1 is the coordinate of the node 1 along axis x_1 , we can approximate the displacement function in each rod element by

$$\mathbf{u} = \mathbf{N}\hat{\mathbf{a}} = \begin{bmatrix} \mathbf{1N} & \mathbf{2N} \end{bmatrix} \begin{Bmatrix} {}^1\hat{\mathbf{a}} \\ {}^2\hat{\mathbf{a}} \end{Bmatrix} \tag{21}$$

where the displacement interpolation matrix is

$${}^1\mathbf{N} = \begin{bmatrix} \phi_1 & 0 & 0 & 0 & 0 & 0 & 0 & 0 \\ 0 & N_1 & 0 & 0 & 0 & N_2 & 0 & 0 \\ 0 & 0 & N_1 & 0 & -N_2 & 0 & 0 & 0 \\ 0 & 0 & 0 & \phi_1 & 0 & 0 & 0 & 0 \\ 0 & 0 & 0 & 0 & 0 & 0 & \phi_1 & 0 \\ 0 & 0 & 0 & 0 & 0 & 0 & 0 & \phi_1 \end{bmatrix} \quad (22)$$

$${}^2\mathbf{N} = \begin{bmatrix} \phi_2 & 0 & 0 & 0 & 0 & 0 & 0 & 0 \\ 0 & N_3 & 0 & 0 & 0 & N_4 & 0 & 0 \\ 0 & 0 & N_3 & 0 & -N_4 & 0 & 0 & 0 \\ 0 & 0 & 0 & \phi_2 & 0 & 0 & 0 & 0 \\ 0 & 0 & 0 & 0 & 0 & 0 & \phi_2 & 0 \\ 0 & 0 & 0 & 0 & 0 & 0 & 0 & \phi_2 \end{bmatrix} \quad (23)$$

$$\mathbf{u} = [u_{10} \quad u_{20} \quad u_{30} \quad \theta_1 \quad \gamma_3 \quad \gamma_2]^T \quad (24)$$

and the displacement vectors of node i in the updated Lagrangian co-rotational frame \mathbf{e}_i of Fig.1 are:

$$\begin{aligned} {}^i\hat{\mathbf{a}} &= [{}^i u_1 \quad {}^i u_2 \quad {}^i u_3 \quad {}^i u_4 \quad {}^i u_5 \quad {}^i u_6 \quad {}^i u_7 \quad {}^i u_8]^T \\ &= [{}^i u_{10} \quad {}^i u_{20} \quad {}^i u_{30} \quad {}^i \theta_1 \quad {}^i \vec{\theta}_2 \quad {}^i \vec{\theta}_3 \quad {}^i \gamma_3 \quad {}^i \gamma_2]^T \quad [i = 1, 2] \end{aligned} \quad (25)$$

where ${}^i \vec{\theta}_2 = -{}^i u_{30,1}$ and ${}^i \vec{\theta}_3 = {}^i u_{20,1}$.

From Eqs.(15) and (21), one can obtain

$$\mathbf{E} = \mathbf{E}^L + \mathbf{E}^N = (\mathbf{B}^L + \hat{\mathbf{B}}^N) \hat{\mathbf{a}} \quad (26)$$

where

$$\mathbf{B}^L = \begin{bmatrix} \phi_{1,1} & 0 & 0 & 0 & 0 & 0 & 0 & 0 \\ 0 & -N_{1,11} & 0 & 0 & 0 & -N_{2,11} & 0 & \phi_{1,1} \\ 0 & 0 & -N_{1,11} & 0 & N_{2,11} & 0 & \phi_{1,1} & 0 \\ 0 & 0 & 0 & \phi_{1,1} & 0 & 0 & 0 & 0 \\ 0 & 0 & 0 & 0 & 0 & 0 & 0 & \phi_1 \\ 0 & 0 & 0 & 0 & 0 & 0 & 0 & \phi_1 \\ \phi_{2,1} & 0 & 0 & 0 & 0 & 0 & 0 & 0 \\ 0 & -N_{3,11} & 0 & 0 & 0 & -N_{4,11} & 0 & \phi_{2,1} \\ 0 & 0 & -N_{3,11} & 0 & N_{4,11} & 0 & \phi_{2,1} & 0 \\ 0 & 0 & 0 & \phi_{2,1} & 0 & 0 & 0 & 0 \\ 0 & 0 & 0 & 0 & 0 & 0 & 0 & \phi_2 \\ 0 & 0 & 0 & 0 & 0 & 0 & \phi_2 & 0 \end{bmatrix} \quad (27)$$

$$\mathbf{G} = \begin{bmatrix} 0 & 0 & 0 & 0 & 0 & 0 & 0 & 0 \\ 0 & N_{1,1} & 0 & 0 & 0 & N_{2,1} & 0 & 0 \\ 0 & 0 & N_{1,1} & 0 & -N_{2,1} & 0 & 0 & 0 \\ 0 & 0 & 0 & 0 & 0 & 0 & 0 & 0 \\ 0 & 0 & 0 & 0 & 0 & 0 & 0 & 0 \\ 0 & 0 & 0 & 0 & 0 & 0 & 0 & 0 \\ 0 & 0 & 0 & 0 & 0 & 0 & 0 & 0 \\ 0 & N_{3,1} & 0 & 0 & 0 & N_{4,1} & 0 & 0 \\ 0 & 0 & N_{3,1} & 0 & -N_{4,1} & 0 & 0 & 0 \\ 0 & 0 & 0 & 0 & 0 & 0 & 0 & 0 \\ 0 & 0 & 0 & 0 & 0 & 0 & 0 & 0 \\ 0 & 0 & 0 & 0 & 0 & 0 & 0 & 0 \end{bmatrix} \quad (28)$$

$$\mathbf{A} = \begin{bmatrix} 0 & u_{20,1} & u_{30,1} & 0 & 0 & 0 \\ 0 & 0 & 0 & 0 & 0 & 0 \\ 0 & 0 & 0 & 0 & 0 & 0 \\ 0 & 0 & 0 & 0 & 0 & 0 \\ 0 & 0 & 0 & 0 & 0 & 0 \\ 0 & 0 & 0 & 0 & 0 & 0 \end{bmatrix} \quad (29)$$

$$\hat{\mathbf{B}}^N = \frac{1}{2} \mathbf{A} \mathbf{G} = \frac{1}{2} \begin{bmatrix} 0 & N_{1,1}u_{20,1} & N_{1,1}u_{30,1} & 0 & -N_{2,1}u_{30,1} & N_{2,1}u_{20,1} & 0 & 0 \\ 0 & 0 & 0 & 0 & 0 & 0 & 0 & 0 \\ 0 & 0 & 0 & 0 & 0 & 0 & 0 & 0 \\ 0 & 0 & 0 & 0 & 0 & 0 & 0 & 0 \\ 0 & 0 & 0 & 0 & 0 & 0 & 0 & 0 \\ 0 & 0 & 0 & 0 & 0 & 0 & 0 & 0 \\ 0 & N_{3,1}u_{20,1} & N_{3,1}u_{30,1} & 0 & -N_{4,1}u_{30,1} & N_{4,1}u_{20,1} & 0 & 0 \\ 0 & 0 & 0 & 0 & 0 & 0 & 0 & 0 \\ 0 & 0 & 0 & 0 & 0 & 0 & 0 & 0 \\ 0 & 0 & 0 & 0 & 0 & 0 & 0 & 0 \\ 0 & 0 & 0 & 0 & 0 & 0 & 0 & 0 \end{bmatrix} \quad (30)$$

and thus

$$\delta(\mathbf{E}) = (\mathbf{B}^L + 2\hat{\mathbf{B}}^N) \delta \hat{\mathbf{a}} = (\mathbf{B}^L + \mathbf{B}^N) \delta(\hat{\mathbf{a}}) = \mathbf{B} \delta \hat{\mathbf{a}} \quad (31)$$

3.2 Updated Lagrangian (U.L.), assumed displacement, weak-formulation of the rod element in the co-rotational reference frame

If τ_{ij}^0 are the initial Cauchy stresses in the updated Lagrangian co-rotational frame \mathbf{e}_i of Fig.1, and S_{ij}^1 are the additional (incremental) second Piola-Kirchhoff stresses in the same updated Lagrangian co-rotational frame with axes \mathbf{e}_i , then the static equations of linear momentum balance and the stress boundary conditions in the frame \mathbf{e}_i are given by

$$\frac{\partial}{\partial x_i} \left[(S_{ik}^1 + \tau_{ik}^0) \left(\delta_{jk} + \frac{\partial u_j}{\partial x_k} \right) \right] + b_j = 0 \quad (32)$$

$$(S_{ik}^1 + \tau_{ik}^0) \left(\delta_{jk} + \frac{\partial u_j}{\partial x_k} \right) n_i - f_j = 0 \quad (33)$$

where b_j are the body forces per unit volume in the current reference state, and f_j are the given boundary loads.

By letting $S_{ik} = S_{ik}^1 + \tau_{ik}^0$, the equivalent weak form of the above equations can be written as

$$\int_V \left\{ \frac{\partial}{\partial x_i} \left[S_{ik} \left(\delta_{jk} + \frac{\partial u_j}{\partial x_k} \right) \right] + b_j \right\} \delta u_j dV - \int_{S_\sigma} \left[S_{ik} \left(\delta_{jk} + \frac{\partial u_j}{\partial x_k} \right) n_i - f_j \right] \delta u_j dS = 0 \quad (34)$$

where δu_j are the test functions.

By integrating by parts the first item of the left side, the above equation can be written as

$$\int_V -S_{ik} \left(\delta_{jk} + \frac{\partial u_j}{\partial x_k} \right) \delta u_{j,i} dV + \int_V b_j \delta u_j dV + \int_{S_\sigma} f_j \delta u_j dS = 0 \quad (35)$$

From Eq.(10) we may write

$$S_{ik}^1 = S_{ik}^{1L} + S_{ik}^{1N} \quad (36)$$

Then the first item of Eq.(35) becomes

$$\begin{aligned} S_{ik} (\delta_{jk} + u_{j,k}) \delta u_{j,i} &= (\tau_{ij}^0 + \tau_{ik}^0 u_{j,k} + S_{ij}^{1L} + S_{ij}^{1N} + S_{ik}^1 u_{j,k}) \delta u_{j,i} \\ &= S_{ij}^{1L} \delta \varepsilon_{ij}^L + \tau_{ik}^0 \delta \left(\frac{1}{2} u_{j,k} u_{j,i} \right) + (\tau_{ij}^0 + S_{ij}^{1N} + S_{ik}^1 u_{j,k}) \delta u_{j,i} \end{aligned} \quad (37)$$

By using Eq.(5), Eq.(35) may be written as

$$\int_V (S_{ij}^{1L} \delta \epsilon_{ij}^L + \tau_{ij}^0 \delta \epsilon_{ij}^N) dV = \int_V b_j \delta u_j dV + \int_{S_\sigma} f_j \delta u_j dS - \int_V (\tau_{ij}^0 + S_{ij}^{1N} + S_{ik}^1 u_{j,k}) \delta \epsilon_{ij}^L dV \quad (38)$$

The terms on the right hand side are ‘correction’ terms in a Newton-Rapson type iterative approach. Carrying out the integration over the cross sectional area of each rod, and using Eqs.(1) to (31), then Eq.(38) can be easily shown to reduce to:

$$\sum_e \left[\delta \hat{\mathbf{a}}^T \int_l (\mathbf{B}^L)^T \mathbf{D} \mathbf{B}^L dl \hat{\mathbf{a}} + \delta \hat{\mathbf{a}}^T \int_l (\mathbf{B}^N)^T \sigma^0 dl \right] = \sum_e \left[\delta \hat{\mathbf{a}}^T \hat{\mathbf{F}}^1 - \delta \hat{\mathbf{a}}^T \int_l (\mathbf{B}^L)^T (\sigma^0 + \sigma^{1N}) dl - \delta \hat{\mathbf{a}}^T \int_l (\mathbf{B}^N)^T \sigma^1 dl \right] \quad (39)$$

where $\hat{\mathbf{F}}^1 = \int_V \mathbf{N}^T \mathbf{b}^* dV + \int_{S_\sigma} \mathbf{N}^T \mathbf{f}^* dS$ is the external equivalent nodal force.

Eq.(39) can be rewritten as

$$\sum_e [\delta \hat{\mathbf{a}}^T (\hat{\mathbf{K}}^L + \hat{\mathbf{K}}^N) \hat{\mathbf{a}}] = \sum_e [\delta \hat{\mathbf{a}}^T (\hat{\mathbf{F}}^1 - \hat{\mathbf{F}}^N)] \quad (40)$$

where $\hat{\mathbf{K}} = \hat{\mathbf{K}}^L + \hat{\mathbf{K}}^N$ is the *symmetric tangent stiffness matrix* of the rod element,

$$\hat{\mathbf{K}}^L = \int_l (\mathbf{B}^L)^T \mathbf{D} \mathbf{B}^L dl \text{ linear part} \quad (41)$$

$$\hat{\mathbf{K}}^N = \int_l (\mathbf{B}^N)^T \sigma^0 dl = \int_l \sigma_1^0 \mathbf{G}^T \mathbf{G} dl \text{ nonlinear part} \quad (42)$$

and

$$\hat{\mathbf{F}}^N = \int_l (\mathbf{B}^L)^T (\sigma^0 + \sigma^{1N}) dl + \int_l (\mathbf{B}^N)^T \sigma^1 dl = \int_0^1 \mathbf{F}_\sigma(\xi) d\xi \quad (43)$$

where $\sigma = \sigma^0 + \sigma^1 = \sigma^0 + \sigma^{1L} + \sigma^{1N}$ are the element generalized stresses.

In this implementation, the linearized σ^1 is employed to update the element stress in the current non-linear step, i.e.,

$$\sigma^1 = \sigma^{1L} = \mathbf{D} \mathbf{B}^L \hat{\mathbf{a}} \quad (44)$$

(47)

where $a_0 = \frac{\sigma_1^0}{l}$, $a_1 = 1.2$, $a_2 = 0.1l$, $a_3 = \frac{2l^2}{15}$, and $a_4 = \frac{-l^2}{30}$.

The symmetric stiffness matrix $\hat{\mathbf{K}}^N$ (16×16), accounts for the interaction of the axial stress in the beam in the co-rotational reference frame, with the continued transverse displacement in the beam in the co-rotational reference frame. In Eq.(47), l is the current length of the beam element in the current reference state with base vectors \mathbf{e}_i , as shown in Fig.1.

$$\hat{\mathbf{K}}^L = \frac{E}{l} \begin{bmatrix} \hat{\mathbf{K}}^{L1} & \hat{\mathbf{K}}^{L12} \\ (\hat{\mathbf{K}}^{L12})^T & \hat{\mathbf{K}}^{L2} \end{bmatrix} \quad (48)$$

where

$$\hat{\mathbf{K}}^{L1} = \begin{bmatrix} A & 0 & 0 & 0 & I_3 & -I_2 & I_3 & I_2 \\ & b_1 & b_2 & 0 & -b_4 & b_5 & 0 & 0 \\ & & b_3 & 0 & -b_6 & b_4 & 0 & 0 \\ & & & b_7 & 0 & 0 & -b_8 & b_9 \\ & & & & 4I_{33} & -4I_{23} & I_{33} & I_{23} \\ & & & & & 4I_{22} & -I_{23} & -I_{22} \\ & & & & & & b_{10} & I_{23} \\ & & & & & & & b_{11} \end{bmatrix} \quad (49)$$

$$\hat{\mathbf{K}}^{L2} = \begin{bmatrix} A & 0 & 0 & 0 & I_3 & -I_2 & I_3 & I_2 \\ & b_1 & b_2 & 0 & b_4 & -b_5 & 0 & 0 \\ & & b_3 & 0 & b_6 & -b_4 & 0 & 0 \\ & & & b_7 & 0 & 0 & b_8 & -b_9 \\ & & & & 4I_{33} & -4I_{23} & I_{33} & I_{23} \\ & & & & & 4I_{22} & -I_{23} & -I_{22} \\ & & & & & & b_{10} & I_{23} \\ & & & & & & & b_{11} \end{bmatrix} \quad (50)$$

$$\hat{\mathbf{K}}^{L12} = \begin{bmatrix} -A & 0 & 0 & 0 & -I_3 & I_2 & -I_3 & -I_2 \\ 0 & -b_1 & -b_2 & 0 & -b_4 & b_5 & 0 & 0 \\ 0 & -b_2 & -b_3 & 0 & -b_6 & b_4 & 0 & 0 \\ 0 & 0 & 0 & -b_7 & 0 & 0 & -b_8 & b_9 \\ -I_3 & b_4 & b_6 & 0 & 2I_{33} & -2I_{23} & -I_{33} & -I_{23} \\ I_2 & -b_5 & -b_4 & 0 & -2I_{23} & 2I_{22} & I_{23} & I_{22} \\ -I_3 & 0 & 0 & b_8 & -I_{33} & I_{23} & -b_{12} & -I_{23} \\ -I_2 & 0 & 0 & -b_9 & -I_{23} & I_{22} & -I_{23} & -b_{13} \end{bmatrix} \quad (51)$$

where $b_1 = 12I_{22}/l^2$, $b_2 = 12I_{23}/l^2$, $b_3 = 12I_{33}/l^2$, $b_4 = 6I_{23}/l$, $b_5 = 6I_{22}/l$, $b_6 = 6I_{33}/l$, $b_7 = \mu I_{rr}/E$, $b_8 = 0.5\mu I_2 l/E$, $b_9 = 0.5\mu I_3 l/E$, $b_{10} = \mu Ak l^2/(3E) + I_{33}$, $b_{11} = \mu Ak l^2/(3E) + I_{22}$, $b_{12} = -\mu Ak l^2/(6E) + I_{33}$, and $b_{13} = -\mu Ak l^2/(6E) + I_{22}$. Thus, $\hat{\mathbf{K}}^L$ is the usual linear symmetric (16×16) stiffness matrix of the beam in the co-rotational reference frame, with the geometric parameters I_2, I_3, I_{22}, I_{33} ,

I_{23} and I_{rr} , and the current length l . If the cross section of the beam is symmetric, $I_2 = I_3 = I_{23} = 0$ and the linear stiffness matrix in Eq.(48) can be simplified.

It is clear from the above procedures, that the present (16×16) symmetric tangent stiffness matrices of the beam in the co-rotational reference frame, based on the simplified rod theory, are much simpler than those based on the exact continuum beam theories of Simo (1985), and Bathe and Bolourchi (1979), or those of Kondoh, Tanaka and Atluri (1986), Kondoh and Atluri (1987), and Shi and Atluri (1988). Moreover, the explicit expressions for the tangent stiffness matrix of each rod can be seen to be derived as text-book examples of nonlinear analyses.

4 Transformation between deformation dependent co-rotational local $[\mathbf{e}_i]$, and the global $[\tilde{\mathbf{e}}_i]$ frames of reference

As shown in Fig.1, \tilde{x}_i ($i = 1, 2, 3$) are the global coordinates with unit basis vectors $\tilde{\mathbf{e}}_i$. \tilde{x}_i and $\tilde{\mathbf{e}}_i$ are the local coordinates for the rod element at the undeformed element. The basis vector $\tilde{\mathbf{e}}_i$ are initially chosen such that (Shi and Atluri 1988)

$$\begin{aligned}\tilde{\mathbf{e}}_1 &= (\Delta\tilde{x}_1\tilde{\mathbf{e}}_1 + \Delta\tilde{x}_2\tilde{\mathbf{e}}_2 + \Delta\tilde{x}_3\tilde{\mathbf{e}}_3)/L \\ \tilde{\mathbf{e}}_2 &= (\tilde{\mathbf{e}}_3 \times \tilde{\mathbf{e}}_1)/|\tilde{\mathbf{e}}_3 \times \tilde{\mathbf{e}}_1| \\ \tilde{\mathbf{e}}_3 &= \tilde{\mathbf{e}}_1 \times \tilde{\mathbf{e}}_2\end{aligned}\tag{52}$$

where $\Delta\tilde{x}_i = \tilde{x}_i^2 - \tilde{x}_i^1$, $L = (\Delta\tilde{x}_1^2 + \Delta\tilde{x}_2^2 + \Delta\tilde{x}_3^2)^{\frac{1}{2}}$.

Then $\tilde{\mathbf{e}}_i$ and $\tilde{\mathbf{e}}_i$ have the following relations:

$$\begin{Bmatrix} \tilde{\mathbf{e}}_1 \\ \tilde{\mathbf{e}}_2 \\ \tilde{\mathbf{e}}_3 \end{Bmatrix} = \begin{bmatrix} \Delta\tilde{x}_1/L & \Delta\tilde{x}_2/L & \Delta\tilde{x}_3/L \\ -\Delta\tilde{x}_2/S & \Delta\tilde{x}_1/S & 0 \\ -\Delta\tilde{x}_1\Delta\tilde{x}_3/(SL) & -\Delta\tilde{x}_2\Delta\tilde{x}_3/(SL) & S/L \end{bmatrix} \begin{Bmatrix} \tilde{\mathbf{e}}_1 \\ \tilde{\mathbf{e}}_2 \\ \tilde{\mathbf{e}}_3 \end{Bmatrix}\tag{53}$$

where $S = (\Delta\tilde{x}_1^2 + \Delta\tilde{x}_2^2)^{\frac{1}{2}}$.

Thus we can define a transformation matrix $\tilde{\lambda}_0$ between $\tilde{\mathbf{e}}_i$ and $\tilde{\mathbf{e}}_i$ as

$$\tilde{\lambda}_0 = \begin{bmatrix} \Delta\tilde{x}_1/L & \Delta\tilde{x}_2/L & \Delta\tilde{x}_3/L \\ -\Delta\tilde{x}_2/S & \Delta\tilde{x}_1/S & 0 \\ -\Delta\tilde{x}_1\Delta\tilde{x}_3/(SL) & -\Delta\tilde{x}_2\Delta\tilde{x}_3/(SL) & S/L \end{bmatrix}\tag{54}$$

When the element is parallel to the \bar{x}_3 axis, $S = [\Delta\bar{x}_1^2 + \Delta\bar{x}_2^2]^{\frac{1}{2}} = 0$ and Eq.(53) is not valid. In this case, the local coordinates is determined by

$$\tilde{\mathbf{e}}_1 = \bar{\mathbf{e}}_3, \tilde{\mathbf{e}}_2 = \bar{\mathbf{e}}_2, \tilde{\mathbf{e}}_3 = -\bar{\mathbf{e}}_1 \tag{55}$$

Let x_i and \mathbf{e}_i be the co-rotational reference coordinates for the deformed rod element. In order to continuously define the local coordinates of the same rod element during the whole range of large deformation, the basis vectors \mathbf{e}_i are chosen such that

$$\begin{aligned} \mathbf{e}_1 &= (\Delta x_1 \bar{\mathbf{e}}_1 + \Delta x_2 \bar{\mathbf{e}}_2 + \Delta x_3 \bar{\mathbf{e}}_3) / l = a_1 \bar{\mathbf{e}}_1 + a_2 \bar{\mathbf{e}}_2 + a_3 \bar{\mathbf{e}}_3 \\ \mathbf{e}_2 &= (\tilde{\mathbf{e}}_3 \times \mathbf{e}_1) / |\tilde{\mathbf{e}}_3 \times \mathbf{e}_1| \\ \mathbf{e}_3 &= \mathbf{e}_1 \times \mathbf{e}_2 \end{aligned} \tag{56}$$

where $\Delta x_i = x_i^2 - x_i^1$, $l = (\Delta x_1^2 + \Delta x_2^2 + \Delta x_3^2)^{\frac{1}{2}}$.

We denote $\tilde{\mathbf{e}}_3$ in Eq.(53) as

$$\tilde{\mathbf{e}}_3 = c_1 \bar{\mathbf{e}}_1 + c_2 \bar{\mathbf{e}}_2 + c_3 \bar{\mathbf{e}}_3 \tag{57}$$

Then \mathbf{e}_i and $\bar{\mathbf{e}}_i$ have the following relations:

$$\begin{Bmatrix} \mathbf{e}_1 \\ \mathbf{e}_2 \\ \mathbf{e}_3 \end{Bmatrix} = \begin{bmatrix} a_1 & a_2 & a_3 \\ b_1 & b_2 & b_3 \\ a_2 b_3 - a_3 b_2 & a_3 b_1 - a_1 b_3 & a_1 b_2 - a_2 b_1 \end{bmatrix} \begin{Bmatrix} \bar{\mathbf{e}}_1 \\ \bar{\mathbf{e}}_2 \\ \bar{\mathbf{e}}_3 \end{Bmatrix} = \lambda_0 \bar{\mathbf{e}}_i \tag{58}$$

where

$$\begin{aligned} b_1 &= (c_2 a_3 - c_3 a_2) / l_{31} \\ b_2 &= (c_3 a_1 - c_1 a_3) / l_{31} \\ b_3 &= (c_1 a_2 - c_2 a_1) / l_{31} \end{aligned} \tag{59}$$

$$l_{31} = [(c_2 a_3 - c_3 a_2)^2 + (c_3 a_1 - c_1 a_3)^2 + (c_1 a_2 - c_2 a_1)^2]^{\frac{1}{2}} \tag{60}$$

and

$$\lambda_0 = \begin{bmatrix} a_1 & a_2 & a_3 \\ b_1 & b_2 & b_3 \\ a_2 b_3 - a_3 b_2 & a_3 b_1 - a_1 b_3 & a_1 b_2 - a_2 b_1 \end{bmatrix} \tag{61}$$

Thus, the transformation matrix λ , between the 16 generalized coordinates in the co-rotational reference frame, and the corresponding 16 coordinates in the global Cartesian reference frame, is given by

$$\lambda = \begin{bmatrix} 1\lambda & \\ & 2\lambda \end{bmatrix} \tag{62}$$

where

$${}^i\lambda = \begin{bmatrix} \lambda_0 & 0 & 0 & 0 \\ 0 & \lambda_0 & 0 & 0 \\ 0 & 0 & b_2 & b_3 \\ 0 & 0 & a_3b_1 - a_1b_3 & a_1b_2 - a_2b_1 \end{bmatrix} \quad (63)$$

Letting x_i and \mathbf{e}_i be the reference coordinates, and repeating the above steps [Eq.(56) – Eq.(63)], the transformation matrix of each incremental step can be obtained in a same way.

If a single straight beam is discretized into finite elements, one may enforce the nodal continuity of $(\vec{\theta}_2$ and $\gamma_2)$ as well as $(\vec{\theta}_3$ and $\gamma_3)$ separately, thus leading to the nodal continuity of the total rotations θ_2 and θ_3 respectively. However, when two or more beams are connected arbitrarily at a node, as in a space-frame, geometric compatibility requires the nodal connectivity of only the global Cartesian components of θ_2 and θ_3 of the beams joined at the node. However, for algebraic simplicity, and with some sacrifice of theoretical exactness, only the nodal connectivity of the global Cartesian components of $(\vec{\theta}_2$ and $\vec{\theta}_3)$ as well as of $(\gamma_2$ and $\gamma_3)$ are enforced separately, in this paper.

Then the element matrices are transformed to the global coordinate system using

$$\bar{\mathbf{a}} = \lambda^T \hat{\mathbf{a}} \quad (64)$$

$$\bar{\mathbf{K}} = \lambda^T \hat{\mathbf{K}} \lambda \quad (65)$$

$$\bar{\mathbf{F}} = \lambda^T \hat{\mathbf{F}} \quad (66)$$

where $\bar{\mathbf{a}}, \bar{\mathbf{K}}, \bar{\mathbf{F}}$ are respectively the generalized nodal displacements, element tangent stiffness matrix and generalized nodal forces, in the global coordinates system.

After assembling the element stiffness matrices and nodal force vectors, into their global counterparts, we obtain the discretized equations of the space frames as

$$\mathbf{Ka} = \mathbf{F} - \mathbf{F}^0 \quad (67)$$

The Newton-Raphson method, modified Newton-Rapson method or the artificial time integration method (Liu 2007a, 2007b; Liu and Atluri 2008) can be employed to solve Eq.(67). In this implementation, the Newton-Raphson algorithm is used.

5 Numerical examples

5.1 A cantilever beam with a symmetric cross section

A large deflection and moderate rotation analysis of a cantilever beam subject to a transverse load at the tip, as shown in Fig. 3, is considered. The cross section of

the beam is a square. The Poisson’s ration is $\nu = 0.25$. The transverse load at the tip is $PL^2/(EI) = 7.0$. The exact linear solution of the vertical tip deflection of the cantilever beam is given by Prathap and Bhashyam (1982) as

$$w_r = \frac{PL^3}{3EI} \left(1 + \frac{3EI}{k\mu AL^2} \right) \tag{68}$$

For the comparison in the following examples, the rod element including the shear deformation is denoted as ‘TKRE’, the rod element not including the shear deformation (Cai, Paik and Atluri 2009a) is denoted as ‘TNRE’, and the two nodal Timoshenko shear flexible beam element with reduced integration is denoted as ‘TSBE’.

Tab.1 shows the comparison of the deflection at the tip for the linear analysis for different ratios of h/L . Tab.2 shows the comparison of the deflection at the tip for the large deformation analysis for different ratios of h/L .

Table 1: Comparison of the deflection (δ/L) at the tip for linear analysis

h/L	0.4	0.2	0.1	0.05	0.02	0.001	0.0001
TNRE	2.33400	2.33300	2.33350	2.33325	2.33330	2.33334	2.33333
TKRE	2.67400	2.41800	2.35450	2.33875	2.33420	2.33334	2.33333
TSBE	2.67800	2.41500	2.34950	2.33300	2.32840	2.32750	2.32750
Exact	2.67000	2.41700	2.35450	2.33850	2.33420	2.33334	2.33333

Table 2: Comparison of the deflection(δ/L) at the tip for nonlinear analysis

h/L	0.4	0.2	0.1	0.05	0.02	0.001	0.0001
TNRE	0.85800	0.79900	0.78500	0.78150	0.78060	0.78042	0.78042
TKRE	0.89800	0.81100	0.78800	0.78225	0.78070	0.78042	0.78042

The results presented in Tab.1 indicate that the present element TKRE has very good characteristics of being free from locking for linear analysis of a rod.

It is shown in Tab.2 that, except for the shear strain, the Poisson’s ration has a little influence to the results of the large deformation analysis of rod (for different ratios of h/L).

5.2 A cantilever beam with an asymmetric cross section

We consider a cantilever beam with an asymmetric cross section, as shown in Fig.4. The Poisson’s ration is $\nu = 0.3$. The areas of cross section in Fig.4 are $A = 1$. The

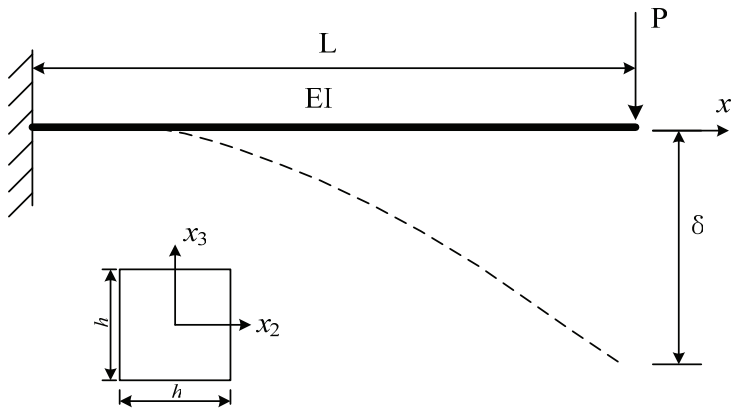


Figure 3: A cantilever beam subject to a transverse load at the tip

transverse load at the tip is $PL^2/(EI_{33}) = 7.0$. Let $h = A^{1/2}$ be the characteristic length of the cross section.

Tab.3 shows the comparison of the deflection u_2/L at the tip for linear analysis for different ratios of h/L . Tab.4 shows the comparison of the deflection u_3/L at the tip for linear analysis for different ratios of h/L .

Table 3: Comparison of the deflection (u_2/L) at the tip for linear analysis

h/L	0.4	0.2	0.1	0.05	0.02	0.001	0.0001
TNRE	3.23600	3.23700	3.23650	3.23650	3.23650	3.23655	3.23650
TKRE	2.54400	3.06300	3.19300	3.22575	3.23480	3.23655	3.23650

Table 4: Comparison of the deflection (u_3/L) at the tip for linear analysis

Table 4: Comparison of the deflection (u_3/L) at the tip for linear analysis

h/L	0.4	0.2	0.1	0.05	0.02	0.001	0.0001
TNRE	5.44200	5.44100	5.44100	5.44100	5.44110	5.44107	5.44100
TKRE	8.92200	6.31100	5.65850	5.49550	5.44980	5.44109	5.44100

Fig. 5 shows the comparison of the deflections in x_3 direction for the cantilever beam with asymmetric cross section by using different rod elements, when $h/L = 0.1$. Fig.6 shows the deflection in x_2 direction for the cantilever beam with asymmetric cross section by using different rod elements, when $h/L = 0.1$. It is noted

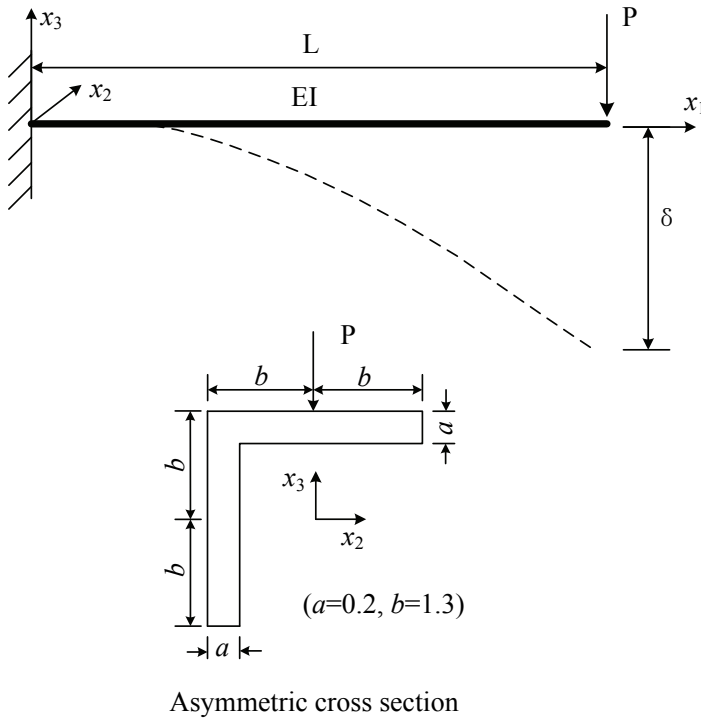


Figure 4: A cantilever beam with an asymmetric cross section

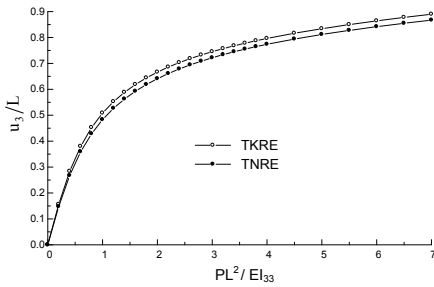


Figure 5: Comparison of the deflections in x_3 direction for the cantilever beam with asymmetric cross section

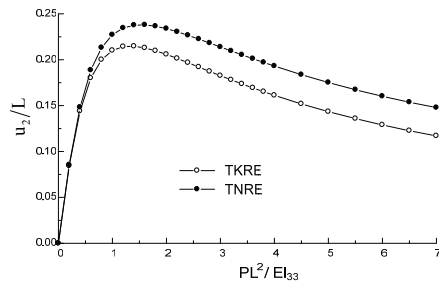


Figure 6: Deflections in x_2 direction for the cantilever beam with asymmetric cross section

that the scale of the abscissa axis should be corrected to $P/2500$ and $E = 0.75e8$ in the same cantilever example with asymmetric cross section in Cai, Paik and Atluri

(2009a, b).

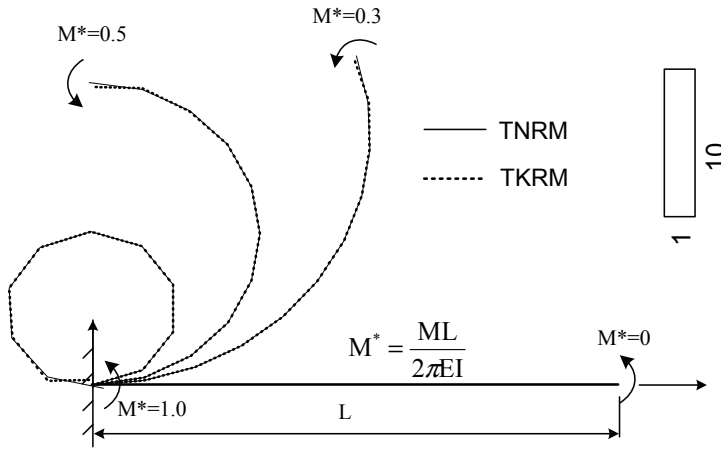


Figure 7: Initial and deformed geometries for cantilever subject to an end-moment by using the thin/thick beam elements ($h/L = 0.1$)

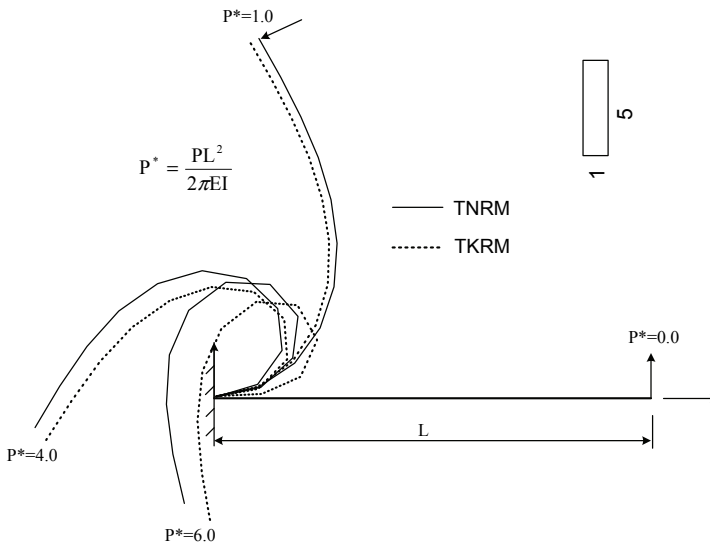


Figure 8: Initial and deformed geometries for cantilever subject to a transverse load by using the thin/thick beam elements ($h/L = 0.2$)

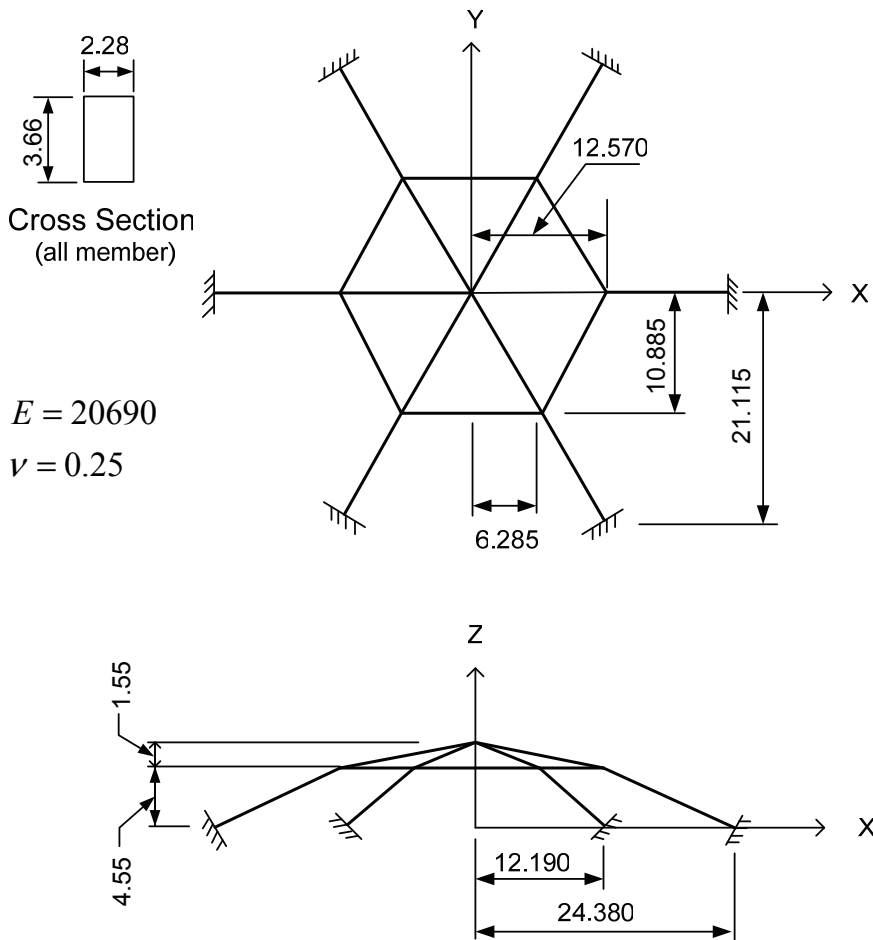


Figure 9: Framed dome

5.3 Large rotations of a cantilever subject to an end-moment and a transverse load

An initially-straight cantilever subject to an end moment $M^* = \frac{ML}{2\pi EI}$ (Crisfield 1990) as shown in Fig.7, is considered. The cross section of the beam is the same as the Fig.3. The beam is divided into 10 equal elements. Fig.6 shows the comparison of the deflections in x_3 direction for the cantilever beam by using the thin/thick beam elements, when $h/L = 0.1$.

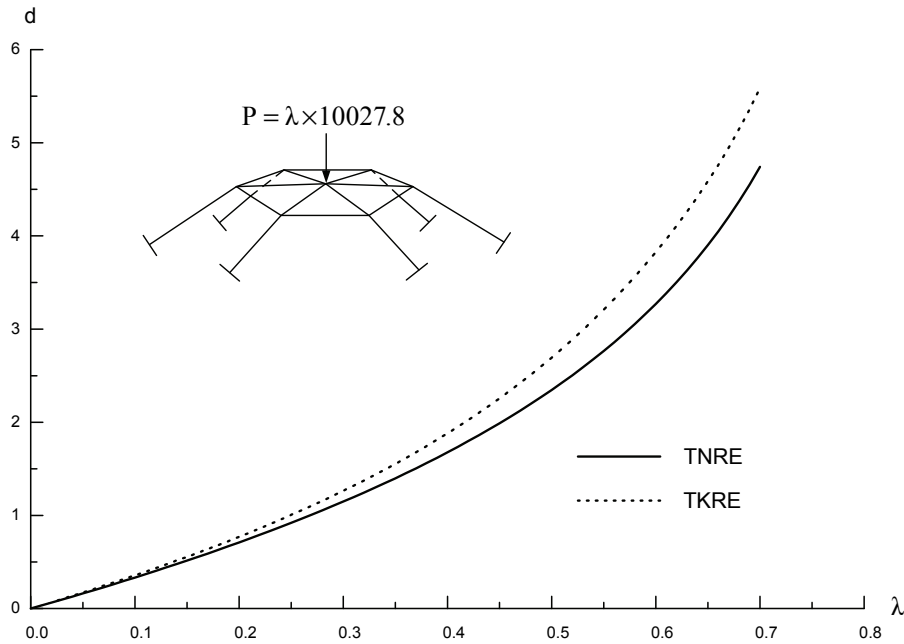


Figure 10: The comparison of the deflections in x_3 direction for the crown point of a framed dome

If a non-conservative, follower-type transverse load $P^* = \frac{PL^2}{2\pi EI}$ is applied at the tip, instead of M^* , the comparison of the deflections in x_3 direction for the cantilever beam by using the thin/thick beam elements, when $h/L = 0.2$, is shown in Fig.8.

5.4 A framed dome

A framed dome shown in Fig.9 is considered (Shi and Atluri 1988). A concentrated vertical load P is applied at the crown point. Each member of the dome is modeled by 4 elements. The comparison of the deflections in x_3 direction at the crown point by using the thin/thick beam elements is shown in Fig.10.

6 Conclusions

Based on a von Karman type nonlinear theory of deformation and the primal principle, a new shear flexible rod/beam element has been developed for large deformation analysis of space frames. The proposed element is simple, economic, and locking free. There is no necessity to separate the bending deformation and shearing deformation, or to employ the reduced/selective integration in this shear flexible

rod element, as in the case of a majority of previous studies. It is shown to be possible to derive an explicit expression for the (16x16) tangent stiffness matrix of each element, including nodal displacements, nodal derivatives of transverse displacements, and nodal transverse shear strains, even if assumed-displacement type formulations are used. The present method can be extended to consider the formation of plastic hinges in each beam of the frame; and also to consider large-rotations of plates and shells.

Acknowledgement: The authors gratefully acknowledge the support of Kwang-Hua Fund for College of Civil Engineering, Tongji University. This research was also supported by the World Class University (WCU) program through the National Research Foundation of Korea funded by the Ministry of Education, Science and Technology (Grant no.: R33-10049). The third author is also pleased to acknowledge the support of the Lloyd's Register Educational Trust (The LRET) which is an independent charity working to achieve advances in transportation, science, engineering and technology education, training and research worldwide for the benefit of all.

References

Atluri, S.N. (1980): On some new general and complementary energy theorems for the rate problems in finite strain, classical elastoplasticity. *Journal of Structural Mechanics*, Vol. 8(1), pp. 61-92.

Atluri, S.N. (1984): Alternate stress and conjugate strain measures, and mixed variational formulations involving rigid rotations, for computational analyses of finitely deformed plates and shells: part-I: theory. *Computers & Structures*, Vol. 18(1), pp. 93-116.

Atluri, S.N. (2005): *Methods of Computer Modeling in Engineering & Science*. Tech Science Press.

Atluri, S.N.; Cazzani, A. (1994): Rotations in computational solid mechanics, invited feature article. *Archives for Computational Methods in Engg.*, ICNME, Barcelona, Spain, Vol 2(1), pp. 49-138.

Atluri, S.N.; Cho, J.Y.; Kim, H.G. (1999): Analysis of thin beams, using the meshless local Petrov-Galerkin method, with generalized moving least squares interpolations. *Computational Mechanics*, Vol 24, pp. 334-347.

Atluri, S.N.; Iura, M.; Vasudevan, S. (2001): A consistent theory of finite stretches and finite rotations, in space-curved beams of arbitrary cross-section. *Computational Mechanics*, vol.27, pp.271-281

Atluri, S.N.; Zhu, T. (1998): A new Meshless Local Petrov-Galerkin (MLPG)

approach in computational mechanics. *Computational Mechanics*, vol.22, pp.117-127

Auricchio, F.; Carotenuto, P.; Reali, A. (2008): On the geometrically exact beam model: A consistent, effective and simple derivation from three-dimensional finite-elasticity. *International Journal of Solids and Structures*, vol.45, pp. 4766–4781.

Bathe, K.J.; Bolourchi, S. (1979): Large displacement analysis of three-dimensional beam structures. *International Journal for Numerical Methods in Engineering*, vol.14, pp.961-986.

Cai, Y.C.; Paik, J.K.; Atluri, S.N. (2009a): Large deformation analyses of space-frame structures, with members of arbitrary cross-section, using explicit tangent stiffness matrices, based on a von Karman type nonlinear theory in rotated reference frames. *CMES: Computer Modeling in Engineering & Sciences*, vol. 53, pp.123-152.

Cai, Y.C.; Paik, J.K.; Atluri, S.N. (2009b): Large deformation analyses of space-frame structures, using explicit tangent stiffness matrices, based on the Reissner variational principle and a von Karman type nonlinear theory in rotated reference frames. *CMES: Computer Modeling in Engineering & Sciences*, vol. 54, pp.335-368.

Chan, S.L. (1996): Large deflection dynamic analysis of space frames. *Computers & Structures*, vol. 58, pp.381-387.

Crisfield, M.A. (1990): A consistent co-rotational formulation for non-linear, three-dimensional, beam-elements. *Computer Methods in Applied Mechanics and Engineering*, vol.81, pp. 131–150.

Dinis, L.W.J.S.; Jorge, R.M.N.; Belinha, J. (2009): Large deformation applications with the radial natural neighbours interpolators. *CMES: Computer Modeling in Engineering & Sciences*, vol.44, pp. 1-34

Gato, C.; Shie, Y. (2008): Numerical Simulations of Dynamic Fracture in Thin Shell Structures. *CMES: Computer Modeling in Engineering & Sciences*, Vol.33, pp. 269-292.

Gendy, A.S.; Saleeb, A.F. (1992): On the finite element analysis of the spatial response of curved beams with arbitrary thin-walled sections. *Computers & Structures*, vol.44, pp.639-652

Han, Z.D.; Rajendran, A.M.; Atluri, S.N. (2005): Meshless Local Petrov- Galerkin (MLPG) approaches for solving nonlinear problems with large deformations and rotations. *CMES: Computer Modeling in Engineering & Sciences*, vol.10, pp. 1-12

Iura, M.; Atluri, S.N. (1988): Dynamic analysis of finitely stretched and rotated 3-dimensional space-curved beams. *Computers & Structures*, Vol. 29, pp.875-889

Izzuddin, B.A. (2001): Conceptual issues in geometrically nonlinear analysis of 3D framed structures. *Computer Methods in Applied Mechanics and Engineering*, vol.191, pp. 1029–1053.

Kondoh, K.; Tanaka, K.; Atluri, S.N. (1986): An explicit expression for the tangent-stiffness of a finitely deformed 3-D beam and its use in the analysis of space frames. *Computers & Structures*, vol.24, pp.253-271.

Kondoh, K.; Atluri, S.N. (1987): Large-deformation, elasto-plastic analysis of frames under nonconservative loading, using explicitly derived tangent stiffnesses based on assumed stresses. *Computational Mechanics*, vol.2, pp.1-25.

Kulikov, G.M.; Plotnikova, S.V. (2008): Finite rotation geometrically exact four-node solid-shell element with seven displacement degrees of freedom. *CMES: Computer Modeling in Engineering & Sciences*, Vol.28, pp. 15-38.

Lee, M.H.; Chen, W.H. (2009): A three-dimensional meshless scheme with background grid for electrostatic-structural analysis. *CMC: Computers Materials & Continua*, vol.11, pp. 59-77

Lee, S.Y.; Lin, S.M.; Lee, C.S.; Lu, S.Y.; Liu, Y.T. (2008): Exact large deflection of beams with nonlinear boundary conditions. *CMES: Computer Modeling in Engineering & Sciences*, vol.30, pp. 27-36

Lee, S.Y.; Lu, S.Y.; Liu, Y.R.; Huang, H.C. (2008): Exact large deflection solutions for Timoshenko beams with nonlinear boundary conditions. *CMES: Computer Modeling in Engineering & Sciences*, vol.33, pp. 293-312

Li, Z.X. (2007): A mixed co-rotational formulation of 2D beam element using vectorial rotational variables. *Communications in Numerical Methods in Engineering*, Vol.23, pp.45–69.

Liu, C.S. (2007a): A modified Trefftz method for two-dimensional Laplace equation considering the domain's characteristic length. *CMES: Computer Modeling in Engineering & Sciences*, vol. 21, pp. 53-66.

Liu, C.S. (2007b): A highly accurate solver for the mixed-boundary potential problem and singular problem in arbitrary plane domain. *CMES: Computer Modeling in Engineering & Sciences*, vol. 20, pp. 111-122.

Liu, C.S.; Atluri, S.N. (2008): A novel time integration method for solving a large system of non-linear algebraic equations. *CMES: Computer Modeling in Engineering & Sciences*, vol.31, pp. 71-83.

Lo, S.H. (1992): Geometrically nonlinear formulation of 3D finite strain beam element with large rotations. *Computers & Structures*, vol.44, pp.147-157

Majorana, C.E.; Salomoni, V.A. (2008): Dynamic Nonlinear Material Behaviour of Thin Shells in Finite Displacements and Rotations. *CMES: Computer Modeling*

in Engineering & Sciences, Vol.33, pp. 49-84.

Mata, P.; Oller, S.; Barbat A.H. (2007): Static analysis of beam structures under nonlinear geometric and constitutive behavior. *Computer Methods in Applied Mechanics and Engineering*, vol.196, pp. 4458–4478.

Mata, P.; Oller, S.; Barbat A.H. (2008): Dynamic analysis of beam structures considering geometric and constitutive nonlinearity. *Computer Methods in Applied Mechanics and Engineering*, vol.197, pp. 857–878.

Mukherjee, S.; Prathap G. (2001): Analysis of shear locking in Timoshenko beam elements using the function space approach. *Communications in Numerical Methods in Engineering*, Vol.17, pp. 385–393.

Prathap, G.; Bhashyam, G.R. (1982): Reduced integration and the shear-flexible beam element. *International Journal for Numerical Methods in Engineering*, vol.18, pp.195-210.

Punch, E.F.; Atluri, S.N. (1984): Development and testing of stable, invariant, isoparametric curvilinear 2-D and 3-D hybrid-stress elements. *Computer Methods in Applied Mechanics and Engineering*, Vol.47, pp.331-356

Reddy, J.N. (1997): On locking-free shear deformable beam finite elements. *Computer Methods in Applied Mechanics and Engineering*, Vol.149, pp.113-132

Simo, J.C. (1985): A finite strain beam formulation. The three-dimensional dynamic problem. Part I. *Computer Methods in Applied Mechanics and Engineering*, vol. 49, pp.55–70.

Shi, G.; Atluri, S.N. (1988): Elasto-plastic large deformation analysis of space-frames: a plastic-hinge and stress-based explicit derivation of tangent stiffnesses. *International Journal for Numerical Methods in Engineering*, vol.26, pp.589-615.

Sladek, J.; Sladek, V.; Solek, P.; Atluri, S.N. (2008): Thermal analysis of Reissner-Mindlin shallow shells with FGM properties by the MLPG. *CMES: Computer Modeling in Engineering & Sciences*, Vol.30, pp. 77-97.

Wen P.H., Hon Y.C. (2007): Geometrically nonlinear analysis of Reissner-Mindlin plate by meshless computation. *CMES: Computer Modeling in Engineering & Sciences*, Vol.21, pp. 177-191.

Wu, T.Y.; Tsai, W.G.; Lee, J.J. (2009): Dynamic elastic-plastic and large deflection analyses of frame structures using motion analysis of structures. *Thin-Walled Structures*, vol.47, pp. 1177- 1190.

Xue, Q.; Meek J.L. (2001): Dynamic response and instability of frame structures. *Computer Methods in Applied Mechanics and Engineering*, vol.190, pp. 5233–5242.

Zhang, C.; Di, S. (2003): New accurate two-noded shear-flexible curved beam

elements. *Computational Mechanics*, Vol.30, pp. 81-87.

Zhou, Z.H.; Chan, S.L. (2004a): Elastoplastic and Large Deflection Analysis of Steel Frames by One Element per Member. I: One Hinge along Member. *Journal of Structural Engineering*, vol. 130, pp.538–544.

Zhou, Z.H.; Chan, S.L. (2004b): Elastoplastic and Large Deflection Analysis of Steel Frames by One Element per Member. II: Three Hinges along Member. *Journal of Structural Engineering*, vol. 130, pp.545–555.

Zhu, T.; Zhang, J.; Atluri, S.N. (1999): A meshless numerical method based on the Local Boundary Integral Equation (LBIE) to solve linear and nonlinear boundary value problems. *Engineering Analysis with Boundary Elements*, vol. 23, pp.375–389.